Boeing's CubeSat TestBed 1 Attitude Determination Design and On-Orbit Experience

Michael Taraba
Primary Author, Former Employee of the Boeing Company

Christian Rayburn; Senior Embedded Software Engineer
Albert Tsuda; Systems Engineer
Charles "Scott" MacGillivray; Program Manager
5301 Bolsa Ave. MC H013-B322, Huntington Beach, CA 92647
christian.g.rayburn@boeing.com
albert.s.tsuda@boeing.com
charles.s.macgillivray@boeing.com

ABSTRACT

The CubeSat standard has provided space access to rapidly accelerate the maturity of hardware components and software algorithms for extremely small satellites. The Boeing CubeSat TestBed 1 (CSTB1) on-orbit experiment, launched April 17, 2007, validated a highly integrated and multi-functional approach for attitude determination. This paper covers the constraints and design concept of a CubeSat attitude determination system using multiple integrated sensors. The on-orbit data collected from five two-axis commercial-off-the-shelf MEMS magnetometers, and four suites of sun sensors was processed and analyzed to determine the attitude of CSTB1. The attitude determination was verified via an image from a low power CMOS camera and solar cell measurements. Lastly, this paper addresses how our attitude determination solution was used to help refine vehicle operations.

INTRODUCTION

Boeing's CubeSat Test Bed 1 (CSTB1) was launched into a 750 km sun-synchronous orbit on April 17, 2007 by an ISC Kosmotras Dnepr rocket from the Baikonur Cosmodrome in Kazakhstan (Reference 1). The primary mission goal of CSTB1 was to accelerate the maturity of CubeSat related components and subsystems, as well as accelerate the general infrastructure and operations of this class of spacecraft.

The CubeSat standard (Reference 2) has enabled low cost access to space by utilizing rideshare opportunities; however, the one kilogram and 10 cm cube definitions have introduced new challenges in satellite design. Most typical, flight qualified, satellite hardware are not compatible due to their mass, power and/or volume requirements; therefore, few attitude sensors exist to provide a three-axis attitude solution for CubeSats. The CSTB1 attitude determination approach utilizes multifunctional elements and commercial-off-the-shelf electronics as a means of providing course attitude knowledge, while addressing the ultra-low size, weight and power constraints.

This paper is structured as follows:

- CubeSat TestBed 1 General Description
- Simple Attitude Determination as Part of Multifunctional Elements
- Simulation Results
- On Orbit Data Analysis
- Conclusions

CUBESAT TESTBED 1 GENERAL DESCRIPTION

The primary mission goals of CSTB1 were to mature and evaluate commercial low power processors, CMOS ultra low power imagers, and associated software algorithms in the space environment, and to provide validation of using integrated attitude determination sensors as part of the multifunctional side panels. Secondary missions included validation of the mission operations center and rapid-prototyping processes in a small team environment.

CSTB1 conforms to the CubeSat standard for a single 1U CubeSat. CSTB1 consists of eight basic functional subsystems: 1) Command and Data Handling, 2) Attitude Determination and Control, 3) Telemetry and Command 4) Electrical Power System, 5) Structure, 6) Mechanisms, 7) Thermal management, and 8) Bus Flight Software. Many of these functional subsystems are physically integrated together as multifunctional elements. For example, the attitude determination sensors and solar cells are integrated on a side panel, PCB boards, which also act as structural elements for CSTB1. Integration of the CSTB1 elements into a 10 cm cube is shown in Figure 1.

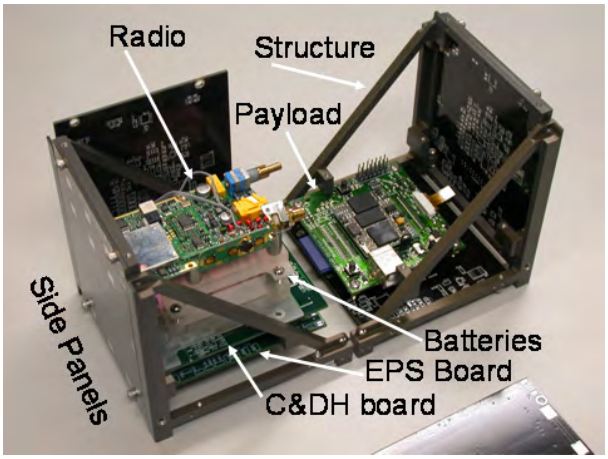

Figure 1: CSTB1 subsystem element integration

SIMPLE ATTITUDE DETERMINATION AS PART OF MULTIFUNCTIONAL ELEMENTS

The attitude determination concept for CSTB1 consisted of four sun sensor suites and five two-axis magnetic sensors integrated into the side panels of the satellite. The goal was to provide enough simple sensor measurements so that a reasonable coarse attitude solution could be derived. Given that four of the six sides of the satellite contain at least two axes of attitude information; course attitude information can be extracted for many attitudes. All sensor data can be directly down linked to the ground for post-processing. The remainder of this section addresses the sensor configuration and attitude determination algorithm used on the ground for post-processing.

CSTB1 Coordinate Frames

The coordinate frame definition in Figure 2 is provided to give a reference when discussing the configuration of the attitude sensors later in this section. The side panels, labeled P0 through P5, are the exposed sides of CSTB1, and each panel normal corresponds to a body axis. Panel 5 (+Z axis) is the payload panel, and the visible color camera is aligned with its panel normal.

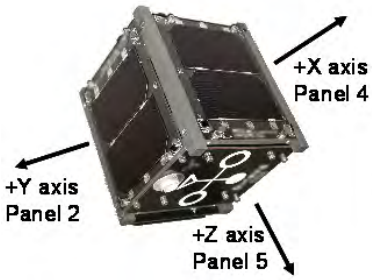

Panel	Body Axis
P0	-Y
P1	-X
P2	+Y
P3	-Z
P4	+X
P5	+Z

Figure 2: CSTB1 Coordinate frame definitions

Sun Sensor Suites

There are four sun sensor suites that provide a measurement of the sun vector in body coordinates, and are located on side panels, P1, P2, P3 and P4. Each sun sensor suite consists of four COTS photodiodes integrated on to the multifunctional side panel, see Figure 3. Each of the four photodiodes is canted 45 degrees from the normal of the side panel board and rotated 90 degrees apart relative to each other to provide 2pi steradian coverage. Their placement on the board is selected to minimize interface from the solar cells and structure of the satellite.

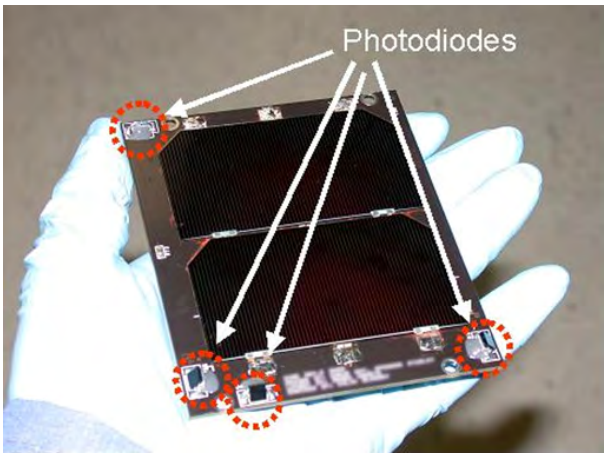

Figure 3: Sun Sensor Suite integrated to Side Panel

Opposing photodiode pairs have overlapping response curves, see Figure 4, and this allows a difference over sums method to define the location of the sun in that axis (Reference 3). For example, assume a panel whose normal is the Z axis, photodiodes 1 & 2 oppose each other (in the X-Z plane) and photodiodes 3 & 4 oppose each other (in the Y-Z plane), the sun vector can then be defined by equation 1. On CSTB1 each sun sensor suite has a different normal vector which corresponds to a body axis; the vector computations are unique for each suite and are defined in equation 2 through 5.

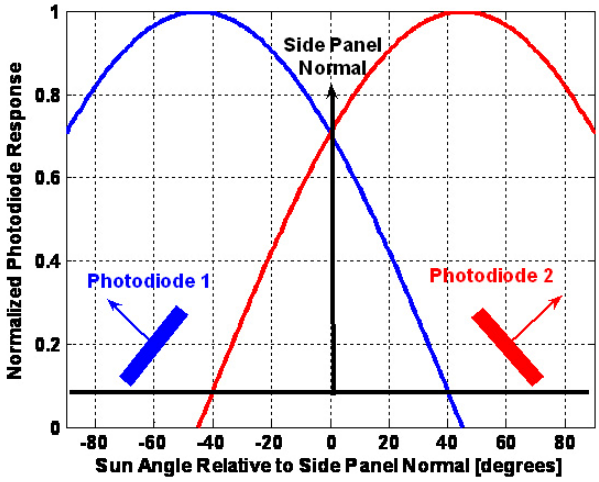

Figure 4: Photodiode Response to Sun Angle

$$SunVector = \begin{bmatrix} \left(\frac{PD_2 - PD_1}{PD_2 + PD_1}\right) \\ \left(\frac{PD_3 - PD_4}{PD_3 + PD_4}\right) \\ 1.0 \end{bmatrix} \quad (1)$$

$$P_1\ SunVector = \begin{bmatrix} -1.0 \\ \left(\frac{PD_3^{P_1} - PD_1^{P_1}}{PD_3^{P_1} + PD_1^{P_1}}\right) \\ \left(\frac{PD_2^{P_1} - PD_4^{P_1}}{PD_2^{P_1} + PD_4^{P_1}}\right) \end{bmatrix} \quad (2)$$

$$P_2\ SunVector = \begin{bmatrix} \left(\frac{PD_3^{P_2} - PD_1^{P_2}}{PD_3^{P_2} + PD_1^{P_2}}\right) \\ 1.0 \\ \left(\frac{PD_2^{P_2} - PD_4^{P_2}}{PD_2^{P_2} + PD_4^{P_2}}\right) \end{bmatrix} \quad (3)$$

$$P_3\ SunVector = \begin{bmatrix} \left(\frac{PD_4^{P_3} - PD_2^{P_3}}{PD_4^{P_3} + PD_2^{P_3}}\right) \\ \left(\frac{PD_3^{P_3} - PD_1^{P_3}}{PD_3^{P_3} + PD_1^{P_3}}\right) \\ -1.0 \end{bmatrix} \quad (4)$$

$$P_4\ SunVector = \begin{bmatrix} 1.0 \\ \left(\frac{PD_3^{P_4} - PD_1^{P_4}}{PD_3^{P_4} + PD_1^{P_4}}\right) \\ \left(\frac{PD_4^{P_4} - PD_2^{P_4}}{PD_4^{P_4} + PD_2^{P_4}}\right) \end{bmatrix} \quad (5)$$

Two-Axis Magnetic Field Sensor

Five of six side panels have a COTS magnetoresistive type two-axis magnetic field sensor. The performance characteristics for the magnetic field sensor are listed in Table 1. Table 2 lists the measured axes for each panel from the magnetic field sensors.

Table 1: Magnetoresistive Chip Characteristics

Characteristic	Units	Value
Noise Density	nV/rt-Hz	50
Resolution	Micro-Gauss	120
Orthogonality	Degrees	0.01
Sensitivity	mV/V/Gauss	1.0

Table 2: Magnetic Field in Body Axes Measured by Each Side Panel

Side Panel	Measured Body Axes
P0	+X
	+Z
P1	-Y
	+Z
P2	-X
	+Z
P3	-Y
	-X
P4	-Y
	-Z

The data from each panel is averaged together to form a single magnetic field sensor measurement providing three axes of information, see equation 6.

$$MagVector = \begin{bmatrix} \left(B_x^{P_0} - B_x^{P_2} - B_x^{P_3}\right)/_3 \\ \left(-B_y^{P_1} - B_y^{P_3} - B_y^{P_4}\right)/_3 \\ \left(B_z^{P_0} + B_z^{P_1} + B_z^{P_2} - B_z^{P_4}\right)/_4 \end{bmatrix} \quad (6)$$

Prior to the launch of CSTB1, the magnetic field sensors were calibrated to the Earth's magnetic field. These sensors were calibrated individually and at the vehicle systems level. In order to compute the offset resulting from integration into the vehicle, magnetic field measurements were taken in two orientations for each panel. Since the largest component of the magnetic field at the location of the test was in a vertical direction, the measurements were taken about this axis. Ideally, the measurements should produce the same magnitude since we are taking measurements of the same field in the opposite directions. The differences in magnitudes were then evaluated to derive sensor offsets and incorporated into the sensor conversions calculations. These sensor conversions were applied prior to executing the attitude determination processing on the ground.

Attitude Determination Algorithm

The attitude determination algorithm was used to help correlate vehicle attitude by using the sun and magnetic field sensor readings downloaded from CSTB1 with images taken from the on-board visible camera. This algorithm statically computes each attitude quaternion estimate based on the available data at that time step. The attitude quaternion estimate computations are based on the TRIAD algorithm (Reference 4), a review below is provided for reference.

The computation of the attitude matrix using TRIAD requires two reference frame unit vectors, $\hat{V}_1$ and $\hat{V}_2$ (in this case Earth Center Inertial is used), and the corresponding measured unit vectors, $\widehat{W}_1$ and $\widehat{W}_2$, in the body frame. The attitude matrix, A, rotates a vector defined in the ECI reference frame to the body reference frame and therefore must satisfy equations 7a & 7b.

$$\widehat{W}_1 = A * \hat{V}_1 \quad (7a)$$

$$\widehat{W}_2 = A * \hat{V}_2 \quad (7b)$$

The algorithm calls for the creation of two sets of column vectors, which are the reference set of vectors given in equations 8 and the measurement set of vectors given in equations 9.

$$\hat{r}_1 = \hat{V}_1 \quad (8a)$$

$$\hat{r}_2 = \frac{(\hat{V}_1 \times \hat{V}_2)}{|\hat{V}_1 \times \hat{V}_2|} \quad (8b)$$

$$\hat{r}_3 = \frac{(\hat{V}_1 \times (\hat{V}_1 \times \hat{V}_2))}{|\hat{V}_1 \times \hat{V}_2|} \quad (8c)$$

$$\hat{s}_1 = \widehat{W}_1 \quad (9a)$$

$$\hat{s}_2 = \frac{(\widehat{W}_1 \times \widehat{W}_2)}{|\widehat{W}_1 \times \widehat{W}_2|} \quad (9b)$$

$$\hat{s}_3 = \frac{(\widehat{W}_1 \times (\widehat{W}_1 \times \widehat{W}_2))}{|\widehat{W}_1 \times \widehat{W}_2|} \quad (9c)$$

The attitude matrix is defined in equation 10.

$$A = \sum_{i=1}^{3} \left(\hat{s}_i \left(\hat{r}_i^{\,T}\right)\right) \quad (10)$$

Since this solution is not symmetric in indices 1 and 2, part of the second measurement vector is discarded, making the attitude estimated more heavily weighted on the first measurement vector. To increase the accuracy of the attitude estimation matrix, the TRIAD solution was augmented with the optimized TRIAD method presented in Reference 5. The optimized TRIAD method computes two attitude matrices: the first, A_1, uses the magnetometer as the first measurement vector, and the second, A_2, uses the sun vector as the first measurement vector. The two attitude estimates are combined based on their respective standard of deviations, σ_1 and σ_2, given in equation 11.

$$A = \frac{{\sigma_1}^2}{{\sigma_1}^2+{\sigma_2}^2}A_1 + \frac{{\sigma_2}^2}{{\sigma_1}^2+{\sigma_2}^2}A_2 \quad (11)$$

The attitude determination algorithm is broken into 4 parts: 1) magnetic field sensor processing, 2) sun sensor processing, 3) TRIAD with valid sun and magnetic field measurements and 4) attitude determination with only magnetic field measurements.

The magnetic field sensor processing is the simplest section which only computes the magnetic field vector based on the sensor readings using equation 6. The sun sensor processing section computes the sun vector for each side panel (P1 through P4) using equations 2-5. Given four sun vectors, a set of deterministic rules is used to determine which sun vector is the most accurate and will be used for attitude determination. 1) The side panel with the greatest number of photodiodes above the minimum threshold is selected as the sun vector. 2) If the side panel with the greatest number of photodiodes only has 1 active photodiode then the sun vector is set to invalid. 3) If none of the photodiodes are active the sun vector is set to invalid.

A 4th part of the attitude determination was created because the satellite has an eclipse period and does not have 4pi steradian coverage with the sun sensors. Therefore, at times, the attitude estimate will not be computable with the standard TRIAD algorithm. This will be discussed later.

The attitude determination uses the optimized TRIAD algorithm when the sun vector is valid. Two attitude matrices are computed, one using the magnetic field vector measurement as the source for the first vector, A_1, and the other using the sun vector measurement as the first vector, A_2. The attitude matrix is then fully computed using information from both attitude matrices according to equation 11. The standard of deviation ratios used are, $\frac{{\sigma_1}^2}{{\sigma_1}^2+{\sigma_2}^2} = 0.6$ and $\frac{{\sigma_2}^2}{{\sigma_1}^2+{\sigma_2}^2} = 0.4$, when a sun vector measurement consists of 4 valid photodiodes. For cases when the sun vector measurement consists of less than 4 photodiodes measurements, then the attitude matrix, A, is set to A_1.

The 4th part of the attitude determination processing was created because the satellite does not have 4pi-steradian coverage with sun sensors during eclipse periods and will result in periods of invalid sun vector measurements. In these cases, the attitude determination method uses only the valid magnetic field vector measurement. This is done by computing the angular rotation between the current magnetic field measurement and the previous magnetic field measurement in equation 12.

$$\theta_{mag} = \cos^{-1}\left(B_{current} \cdot B_{previous}\right) \quad (12)$$

Next, the direction of the magnetic field rotation is computed in equation 13.

$$\hat{e}_{mag} = \frac{\left(\hat{B}_{current} \times \hat{B}_{previous}\right)}{\left|\left(\hat{B}_{current} \times \hat{B}_{previous}\right)\right|} \quad (13)$$

The delta quaternion to the current attitude estimate is then computed in equation 14.

$$\delta\hat{q}_{est} = \begin{bmatrix} \hat{e}_{mag} \sin\left({\theta_{mag}}/{2}\right) \\ \cos\left({\theta_{mag}}/{2}\right) \end{bmatrix} \quad (14)$$

The delta quaternion estimate is combined with the previous estimate to compute the current attitude estimate in equation 15.

$$\hat{q}_{est} = \hat{q}_{est} \otimes \delta\hat{q}_{est} \quad (15)$$

However, this solution is not accurate as it will be missing information in one axis and will be susceptible to significant attitude drift. For the intended purpose of CSTB1, this solution will suffice.

SIMULATION RESULTS

The initial validation of the CSTB1 attitude determination algorithms were simulated using MATLAB. The simulation included key elements necessary to validate the attitude determination: orbital and spacecraft dynamics models, a magnetic field model, math models of the magnetic field, and sun sensors including noise terms and misalignments.

Multiple simulation cases were evaluated to determine an average expected performance of the attitude determination algorithm based on CSTB1's configuration. Nine specific scenarios of performance were examined in the simulation. For each scenario provided in Table 3, the satellite rotates about a vector at varying tumble rates with correlating sun vector measurement unavailability.

Table 3: CSTB1 Attitude Determination Simulations

Case	Satellite Rate [deg/sec]	%Sun Sensor Unavailability
1	0.5	0
2	0.5	30
3	0.5	75
4	0.25	0
5	0.25	30
6	0.25	75
7	0.1	0
8	0.1	30
9	0.1	75

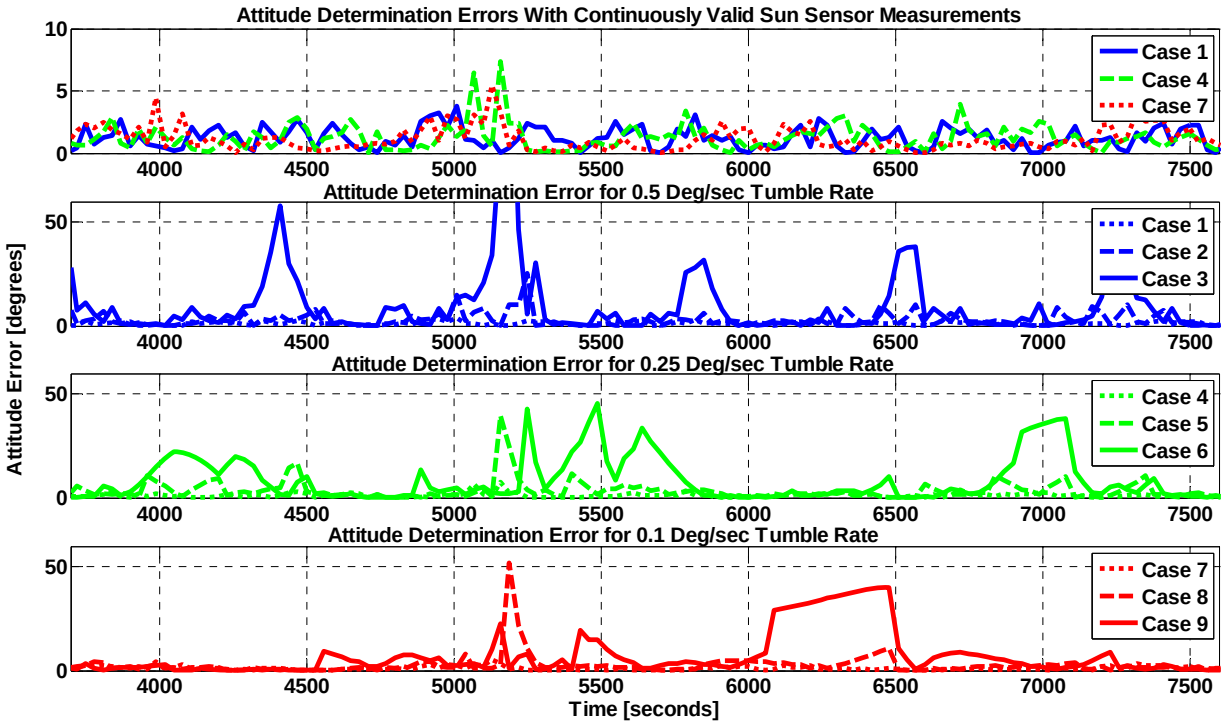

Figure 5: Simulation Attitude Error for Evaluated Cases

The simulation results shown in Figure 5 demonstrate the varying accuracy and sensitivity of the algorithm to sensor characteristics and satellite tumble rates. The attitude accuracy is impacted by two elements: invalid sun vector measurements and satellite tumble rate. The attitude accuracy is less than five degrees during periods of continuously valid sun vector measurements. The increasing magnitude of the tumble rate increases the magnitude of the attitude error when the tumble rate causes outages in the sun vector measurement.

ON-ORBIT DATA ANALYSIS

CSTB1 was launch on April 17, 2007 into a 745 km sun-synchronous orbit. On-orbit operational life has resulted in over one million various sensor data points and 50 images. The flight data presented here represents a 90-minute snapshot of one orbit of CSTB1 on June 17, 2007. This sequence of data is used to draw valuable information regarding the attitude determination system, and how the satellite is tumbling. The measurements from the sun sensors on panel 1 (Figure 6) show that the sensors saturate quickly when exposed to the sun. As a result, much of the valuable angular data that can be extracted from the sun vector was lost.

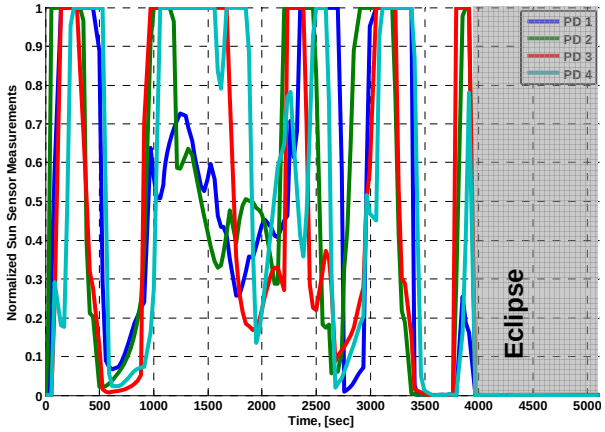

Figure 6: Normalized Sun Sensor Suite measurements from Panel 1

The magnetic field sensors measurements in Figure 7 are the calibrated measurement values. Two of the field measurements provided incorrect readings, the side panel P_0 X sensor and side panel P_2 Z sensor, which were not used in the attitude determination. The information also indicates that the vehicle attitude is oscillating relative to the magnetic field of the Earth. It is suspected that the significant magnetic moment created by the ¼ wave dipole antenna had aligned with the earth's magnetic field and the satellite was oscillating about it. The fact that the satellite had a strong moment that aligned with the magnetic field, allowed operation of CSTB1 to coarsely predict where the payload panel would be facing for operations of the visible camera.

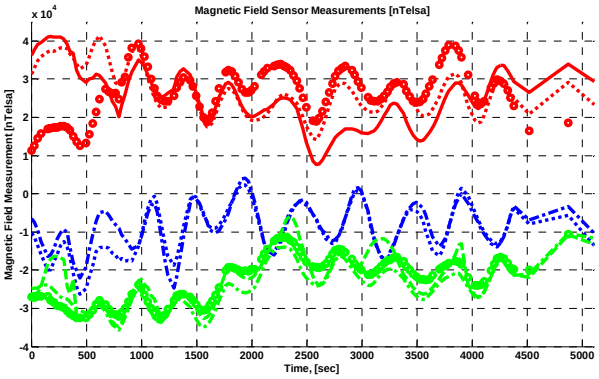

Figure 7: Calibrated Magnetometer Measurements

The attitude determination algorithm was run against the flight data over the 90-minute period shown in Figure 8.

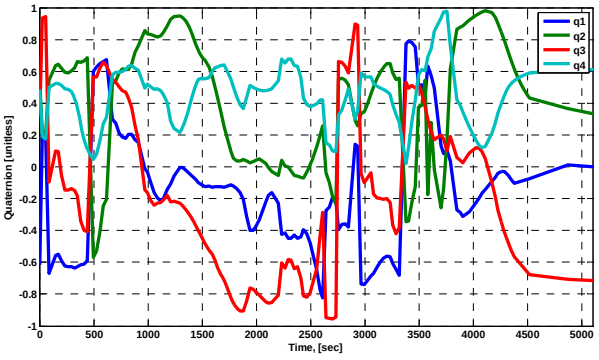

Figure 8: Computed Attitude determination Quaternion

The image in Figure 9 was scheduled and captured from CSTB1 and was used as a source to validate the attitude determination estimate. The image clearly

shows several significant Earth landmarks, which include lakes, the Himalayan mountain range and Mount Everest. In order to determine which landmarks are in the image and the accuracy of the attitude determination solution, we computed where the camera was pointed at the time the image was taken. The latitude and longitude of the subsatellite point (46.9N, 94.5E) and the unit vector of the Z axis acquired from the attitude determination are used to determine the latitude and longitude of the image. The computed angle between the Z axis and nadir is 16.7 degrees which results in a latitude and longitude for the image of 33.4 degrees North latitude and 81.8 degrees East longitude. The USGS Global Visualization Viewer (Reference 6) was used to identify the lake and mountain range landmarks from a LandSat 7 image from April 2007, as shown in Figure 10. The green outline in the LandSat 7 imagery represents the area imaged by CSTB1. The landmarks located at 29 degrees North latitude and 85.6 degrees East longitude are also outlined in the image for clarity. Based on the image latitude and longitude from the USGS, the pointing angle off nadir was determined to be 18.9 degrees. This demonstrated a 2.2 degree error in the attitude determination solution from CSTB1.

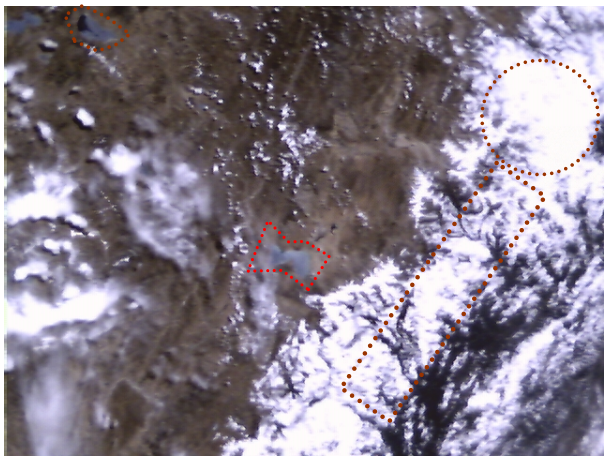

Figure 9: Image captured by Low Power Imager on 17 June 2007 (red outlines are key landmarks identified on the comparison image)

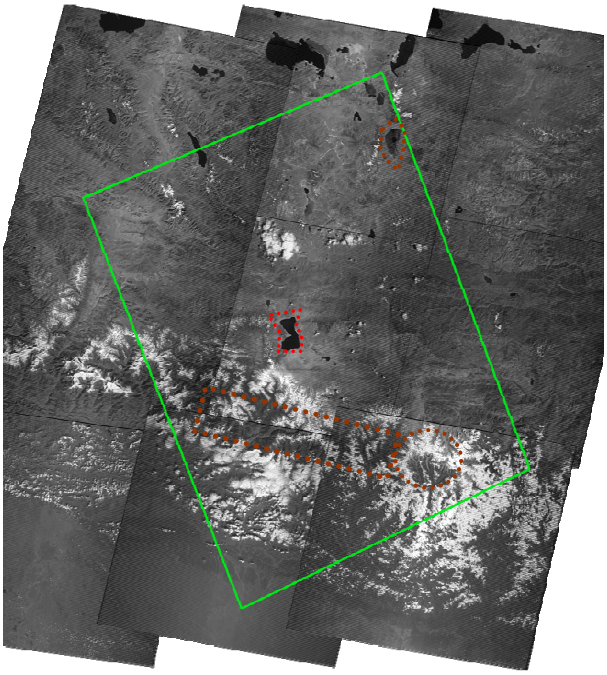

Figure 10: USGS Comparison Image, Green outline represents the CSTB1 Image, Red outlines are the corresponding identifying landmarks

CONCLUSIONS

This paper demonstrated how simple, highly integrated, commercial-off-the-shelf components can be used for CubeSat attitude determination. The optimized TRIAD algorithm implemented on the ground used the sun sensor suites and magnetic field sensors data to determine the satellite attitude and verify the location of an earth image taken by CSTB1's camera. The magnetic field sensors proved to be the most useful of all the sensors because of their high availability. Attitude estimates derived for CSTB1 sensor data was used to determine the impact of the magnetic dipole created by CSTB1 antenna. This allowed ground operators to coarsely predict the pointing direction of the on-board camera and schedule collections of imagery over areas of interest.

Boeing's CSTB1 CubeSat has successfully completed all primary and numerous secondary mission objectives, and has provided extremely useful data throughout its 20+ months on orbit.

ACKNOWLEDGMENTS

The authors would like to thank all the various people who contributed to the success of CSTB1. Specifically, we would like to thank Arthur "Frank" Cooper, Chris Day, Dan Minear, Phil Reid, Thanh Tang, and Doug Yarbrough for all their dedication this to project.

REFERENCES

1. CubeSat Community Website, http://cubesat.atl.calpoly.edu/pages/missions/dnepr-launch-2.php

2. CubeSat Design Specification REV. 11, http://cubesat.atl.calpoly.edu/media/CDS_rev11.pdf

3. Larson, W.J. and J.R. Wertz, "Space Mission Analysis and Design, 3rd Ed." Microcosm Press, October 1999.

4. Shuster, M.D. and S.D. Oh, "Three-Axis Attitude Determination from Vector Observations". AIAA Journal Guidance and Control, Vol. 4, No. 1, January-February 1981, pp. 70-77.

5. Itzhack, B.Y. and R.R. Harman, "Optimized TRIAD algorithm for attitude determination". AIAA/AAS Astrodynamics Conference, San Diego, CA, July 1996. pp. 422-427.

6. USGS Global Visualization Viewer, http://glovis.usgs.gov